Impact de la force ionique, des caractéristiques du milieu poreux et des forces de traînées sur le transport d'E. coli analysé par imagerie confocale

Le chapitre 3 correspond à un article soumis à la revue Environmental Science and Technology

Impact of Ionic Strength, drag force and Porous media characteristics on *Escherichia coli* transport analyzed by *in situ* fluorescens time lapse confocal imaging.

A. Jacobs, R. Briandet et F. Lafolie

Avant propos

Le chapitre 2 a montré l'importance des caractéristiques physicochimiques de la surface cellulaire sur l'adhésion et le déplacement de bactéries dans du sable. Les bactéries hydrophiles et fortement chargées négativement sont les mieux transportées. La souche *E. coli* PHL1314 a présenté une des meilleures capacités de déplacement dans le sable parmi toutes les bactéries étudiées. Cette souche sera donc utilisée pour la suite de l'étude d'autant plus qu'il s'agit d'un bon indicateur de contamination fécale. Mais la partie discussion du chapitre 2, tout comme la littérature suggère que les interactions physicochimiques ne sont pas seules à influer sur le transport bactérien en milieu poreux. De nombreux auteurs supposent également l'importance des phénomènes de blocage des cellules dans une matrice porale et les effets des forces hydrodynamiques. Aussi nous avons voulu mieux comprendre et vérifier le phénomène de blocage physique des cellules dans un milieu poreux en visualisant ce phénomène par des techniques de microscopie confocale. Nous avons ainsi pu observer l'attachement et le détachement des cellules ainsi que leur rétention par blocage physique. L'effet de la morphologie irrégulière des grains de sables sur le transport bactérien a été mis en évidence par comparaison avec des billes de verres parfaitement sphériques. Les forces de traînées hydrodynamiques ont été évaluées et leur influence sur la rétention ou le détachement dans un pore discuté. Enfin nous avons étudié le transport de la souche PHL1314 en présence et en absence d'une barrière électrostatique en variant la force ionique de l'environnement.

Abstract

Bacterial transport through porous media has received increasing attention because of its implication in drinking water contamination and bioremediation applications. In the present study *Escherichia coli* PHL1314 transport through sand and glass porous media in different ionic strength (IS) was investigated. Competition between electrostatic interactions, Lifshitz-van der Waals (referred as the secondary minimum) and drag forces were analysed. Classical column experiments were complemented by *in situ* confocal microscope observations to visualize bacterial cell behaviour inside the porous media. Both the PHL1314 strain and the porous media used were negatively charged and as a result repel each other. Transport was negligible at 10^{-1}M NaCl while 89% and 95% of the *E. coli* cells were transported at 10^{-2}M NaCl through the sand and the glass matrix respectively. In 10^{-1}M solution the secondary minimum is stronger (-3.69kT) than the minimum drag forces (3.31kT) creating favourable conditions for bacterial retention. On the contrary in lower ionic environment the secondary minimum is weakened and bacterial retention is less likely. Decreasing the IS by injecting successively lower ionic solutions starting from 10^{-1}M NaCl caused 18% and 40% of the cells to be released from the secondary minimum for the sand and the glass columns respectively. It come into sight that the electrostatic barrier thickness was responsible for the release of the PHL1314 strain in porous media as it increased dramatically from 4nm to 400nm and caused the secondary minimum to be attenuated. Irreversibly retained bacteria were likely blocked by other phenomena such as wedging or surface roughness as the confocal microscope observations pointed out. In situ time lapse fluorescens imaging demonstrated how particle geometry of sand grains was more likely to trap and retain bacterial cells than smooth glass beads. These results confirm the importance of electrostatic interactions in bacterial transport through porous media phenomena but also the impact of porous media outline characteristics.

1. Introduction

Bacterial transport through porous media is an important issue in environmental stakes such as bioremediation or protecting drinking water sources (Fontes *et al.* 1991). *Escherichia coli* presence in ground water is a common indicator for faecal contamination (Tian *et al.* 2002) and understanding its transport in subsurface environments is of great interest in preventing water wells from harmful contamination (Krapac *et al.* 2002; Unc et Goss 2004). Bacterial transport has commonly been studied with the colloid filtration theory (Yao 1971) based on laboratory and field scale experimental data (Brown et Abramson 2006). According to Yao's conceptual model retention of colloids in porous media is the result of mass transfer from the bulk fluid to the collector grains surface controlled by interception, sedimentation and diffusion mechanics. Bacterial transport is predicted with the classical colloid filtration theory by calculating the anticipated rate of adhesion k_d which is dependent on porous media porosity, fluid flow velocity, collectors grain diameter and single-collector contact efficiency (η_0) (*6*). Recently Tufenkji and Elimelech provided an updated equation to calculate η_0 (Tufenkji et Elimelech 2004). But in unfavorable conditions (i.e. presence of repulsive energy between colloids and porous marix) the deposition coefficient is largely reduced (Cail et Hochella 2005; Li *et al.* 2005). In fact most bacterial cells (or colloids) and sediments are typically negatively charged at groundwater low ionic strength and mild pH resulting in electrostatic repulsions occurring between bacterial cells and soil particles and so creating unfavorable conditions for deposition. Despite repulsive energy several authors found colloid deposition occurred nevertheless (Cail et Hochella 2005; Liu *et al.* 2007; Tong et Johnson 2006). Several discrepancies between experimental data and colloid transport predicted by theories like DLVO or clean bed filtration were presumably caused by surface roughness (Bhattacharjee *et al.* 1998; Bhattacharjee *et al.* 1998; Shellenberger et Logan 2002), hydrodynamics (Bergendahl et Grasso 2000; Li *et al.* 2005) and colloid detachment. Colloid detachment from packed beds has received significant attention although bacterial detachment received less interest (Rijnaarts *et al.* 1996).

In fact bacterial transport is complexed due to the living nature of microbes (Abu-Lail et Camesano 2003). Moreover porous media are too much idealized for practical reasons causing bacterial deposition to be underestimated. Multiple mechanisms like the secondary minimum (Redman *et al.* 2004), zones of flow stagnation (Johnson *et al.* 2007), surface charge and heterogeneity (Li et Logan 2004; Vadillo-Rodriguez et Logan 2006) may create locally favorable deposition conditions complicating bacterial transport predictions. Johnson and colleagues simulated colloids behaviour at a microscale in a porous media by means of a model accounting for the various forces experienced by the particles (Johnson *et al.* 2007). They showed that colloid retention in presence of an energy barrier could happen due to wedging and retention in zones of flow stagnation (Johnson *et al.* 2007). In other work Jonhson *et al*. found that colloid retention in porous media was much higher than in a jet impulse system suggesting porous media structure effects on colloid retention (Tong et Johnson 2006). However the impact of porous matrix effects on bacterial transport is still badly understood and needs further investigation.

The global aim of the study was to bring some insights in the attachment and detachment phenomena of a bacterial cell (*E. coli*.) transported in a porous medium. We carried out bacterial transport experiments in columns filled with two material (sand or glass beads) having similar size and surface charges but differing by their roughness and geometry. In complement an original experimental setup using micro-flowcells, genetically engineered fluorescent *E. coli* cells and fluorescens in situ time lapse confocal imaging made spatial and temporal visualization of the attachment and detachment phenomena possible. Favourable and unfavourable conditions were used for deposition experiments. For detachment, the ionic strength of the solution was progressively lowered. Filtration theory, DLVO theory and the drag forces experienced by the cells are considered when analysing the results. Results are also analyzed in light of recent mechanistic simulations on colloids retention in porous medium (Johnson *et al.* 2007) .

2. Material and Methods

2.1. Strain, plasmid and fluorescent labeling

The bacterial strain used in this study was *Escherichia coli* K12 MG1655 *ompR234* (Vidal *et al.* 1998) (PHL1314) and was kindly given by P. Lejeune (French Institute of Applied Science, Lyon, FRANCE). This strain was selected for its astonishing mobility capacities in porous media as described previously (Jacobs *et al.* 2007). PHL1314 transport behavior was presumably due to the hydrophilic negatively charged outer cell surface characteristics (Jacobs *et al.* 2007). The *E. coli* strain used in this study was genetically fluorescently labeled using the pDsred-express plasmid (Clonetech, USA). Cells were transformed using the chemical TSS method (Transformation Storage Solution: PEG3350 10%, $MgCl_2$ 10mM, $MgSO_4$ 10mM, DMSO 5%). The pDsred-express plasmid inserted is carrying the *dsred* gene witch encodes for the red fluorescent protein from *Discosoma* sp. reef coral. Dsred maximum excitation wavelength is 556nm and maximum emission is 586nm. The bacterial cells were fluorescently labeled in order to perform cytometry counting and in situ confocal imaging. The pDsred-express plasmid also provides resistance to ampicillin antibiotic. Prior experiments, bacteria were cultivated overnight in 100ml of half diluted Luria Bertani media at 30°C, 100rpm. 100mg.L^{-1} of ampicillin was added to ensure the selection of cells carrying the pDsred-express plasmid.

2.2. The electrostatic free energy of interaction.

To be able to quantify the influence of ionic strength on bacterial interaction with the porous media the electrostatic free energy of interaction from the classical DLVO theory was calculated. The DLVO theory also includes Lifshitz-van der Waals interactions and has been calculated in our previous study (Jacobs *et al.* 2007). Although a raw approximation, for practical reasons we consider porous media grains as flat plates and the bacteria as spherical colloids since porous media grains are at least 100 times greater than bacterial cells. The electrostatic interaction free energy as a function of distance *y* between a spherical bacterium (1), and a flat plate (2), immersed in water (3)

Characteristics	Glass beads	Sand
Grain Size (µm)	250	230-310
Manufacturer	Merck	Merck
Column volume (cm^3)	294,5	294,5
Dry solid mass(g)	455	480
Density ($g.cm^3$)	2,5	2,65
Column density ($g.cm^3$)	1,54	1,63
Porosity	0,382	0,385
Pore Volume (cm^3)	112,5	113,4
N_{pore}	$2.24e10^4$	NC
d_c (m)	$9.74e10^{-5}$	NC
d_{max} (m)	$2.09e10^{-4}$	NC
Pump flow ($cm.ml^{-1}$)	3,01	3,03

Table 1: Porous media and column characteristics

NaCl ($mol.L^{-1}$)	PHL1314 strain	glass beads	sand
10^{-1}	-23	-18	-17
10^{-2}	-48	-41	-42
10^{-3}	-55	-46	-48
10^{-4}	-65	-50	-51

Table 2: Results of potential zeta (mV) measurements for porous media and the PHL1314 strain for different ionic strengths

Ionic strength ($mol.l^{-1}$)	Sand			Glass beads		
	V/Vp	BTR (%)	SD (%)	V/Vp	BTR (%)	SD (%)
10^{-2}	0	**89,8**	2,75	0	**94,93**	4,34
10^{-1}	0	**0**	0	0	**0,8**	0.06
10^{-2} (*)	1,15	1,3		1,77	2,0	
10^{-3} (*)	3,01	4,8		3,54	13,9	
10^{-4} (*)	5,36	7,1		5,32	13,0	
Distilled Water (*)	7,62	5,1		7,08	10,9	
total (*)		**18,2**			**40,5**	

Table 3: Bacterial transport rate (BTR) obtained at different ionic strengths with both sand and glass column experiences.

(*) corresponds to the experiences with decreasing ionic strengths inside the columns starting from 10^{-1} $mol.l^{-1}$. Moments of injections are expressed in pore volumes (V/Vp).

can be calculated from (Chen et Strevett 2002). ζ potentials (V) of bacteria were determined by micro-electrophoresis using a Zetaphoremeter model (II) (CAD Instrumentation, Limours, France). The electrophoretic mobility was measured with the bacteria collected after overnight culture, suspended in either 10^{-1}M, 10^{-2}M, 10^{-3}M and 10^{-4}M NaCl solutions at pH7. Bacterial cells were placed in a measurement cell under a microscope equipped with a CCD camera. Their displacements in response to an applied electric field of 8V.cm^{-1} were recorded and the velocity of individual cells was calculated. The ζ potentials were calculated with the conventional Smoluchowski theory for each cell. The displacements of about one hundred cells were recorded at each measurement. The experiment was repeated three times from separate cultures for every ionic strength.

The electro kinetic properties of the sand and the glass beads were measured by a streaming potential analyzer Zetacad (CAD Instrumentation, Limours, France) in a either 10^{-1}M, 10^{-2}M, 10^{-3}M and 10^{-4}M NaCl solutions at pH7. The zeta potential was calculated from the streaming potential experiments as described by Elimelech *et al.* (Elimelech *et al.* 2000).

2.3. Column experiments.

The experimental setup consisted in Plexiglas columns (Ø = 50mm, length = 150mm) filled either with clean sand or glass beads. Porosity and porous media characteristics are listed in table 1. The sand used in this study is called “sand of Fontainebleau” (south Paris, France) and is very homogeneous (over 99.6% silica). Before use, both porous media were thoroughly rinsed with milliQ water on a 40µm filter (VWR international, 11cm, type 417) then sterilized and oven dried for at least 2 hours at 120°C. Next the columns were saturated with sterilized water (10^{-1}M or 10^{-2}M NaCl pH7). For each experiment porous media were renewed in the columns.

Bacterial cells were collected after overnight culture, centrifuged for 5min at 5000tr/min and suspended in a sterile 10^{-1}M or 10^{-2}M NaCl pH7 solution. Before use, concentration of the bacterial solution was adjusted approximatively to 5.10^7 cells/ml. Injection of the bacteria in the column lasted 10 minutes at the approximate flow rate of 3 mL.min^{-1} (flow rates are listed in table 1). Circulation of the bacteria through the column was obtained by mean of a peristaltic pump (Ismatec SA reglo digital MS-4,

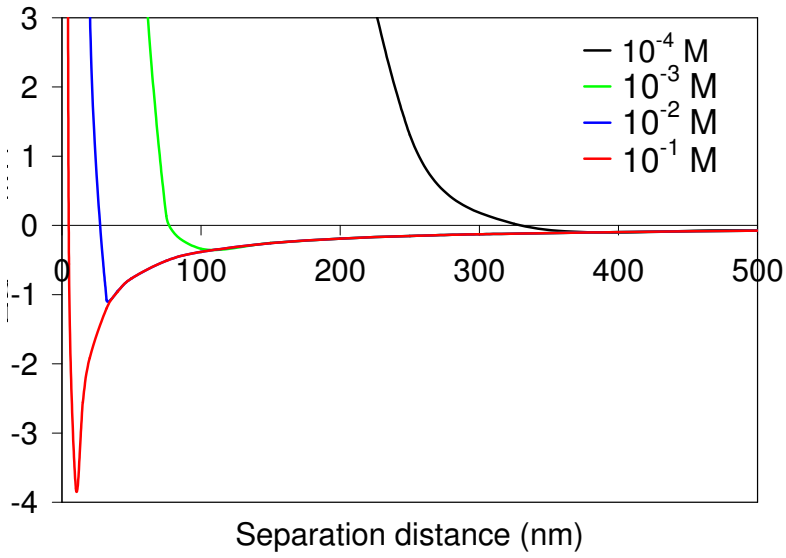

Figure 1: Free energy of interaction as a function of distance between sand and the PHL1314 strain in different ionic strengths (mol.l^{-1}), calculated according to the classical DLVO theory.

Attraction occurs when ΔG is negative, repulsion occurs when ΔG is positive.

Switzerland). Each column experiment was repeated four times with bacteria cells from separate cultures. Experiments were also carried out with decreasing the ionic strength (IS) of NaCl (10^{-1}M, 10^{-2}M, 10^{-3}M, 10^{-4}M and finally milliQ water). These experiments were repeated two times with cells from independent cultures for both the sand and the glass beads columns. Times of IS change of injected solutions are listed in table 3 (indicated in pore volumes). Bacterial concentration was measured by taking 0.5ml samples at the outlet of the column for flow cytometer enumeration. The flow cytometer (Beckman Coulter, EPIC XL, Fullerton, USA) settings were as follows: excitation source 488nm, fluorescence detection on FL2 channel (emission 510-530nm), analysis time 1 minute, no compensation was used.

2.4. Fluorence time lapse confocal imaging

Bacterial displacement through the two porous media (sand and glass beads) was observed with a LEICA SP2 AOBS spectral confocal microscope (Leica Microsystems, France) at the MIMA2 microscopic plateform (http://voxel.jouy.inra.fr/mima2). A single channel micro-flowcell (length: 50mm volume: 250mm^3, Ibidi, Germany) was filled with sand or glass beads and connected to a peristaltic pump (Watson-Marlow, serie200, UK) running at 8.5µL.min^{-1} to obtain about the same flow rate as in the column experiments. The fluid running through the porous media was a pH7 10^{-1}M or 10^{-2}M NaCl solution to visualize IS effect on bacterial adhesion/detachment phenomena. Once the bacteria were attached to the matrix with 10^{-1}M NaCl solution, distilled water was also injected in the flow cell. Bacterial concentration of the injected solution was approximatively 10^6cells.ml^{-1}. Since both sand particles and glass beads are not fluorescent FITC was added to the bulk fluid when necessary to create a negative fluorescent staining. FITC is a green fluorescent molecule with maximum excited/emission wavelengths of 506/529nm. For time lapse series, a fluorescent picture was taken every 3 seconds from a same field to view the dynamic of bacterial adhesion/detachment process *in situ* and in real time. We also looked for specific sites favorable for adhesion and wedging in both porous media such as particle-particle junctions, dead end paths or cell scale furrows were bacteria might be trapped. LSClite v2.5 software (Leica Microsystems, Germany) was used to quantify the fluorescence from the time series obtained.

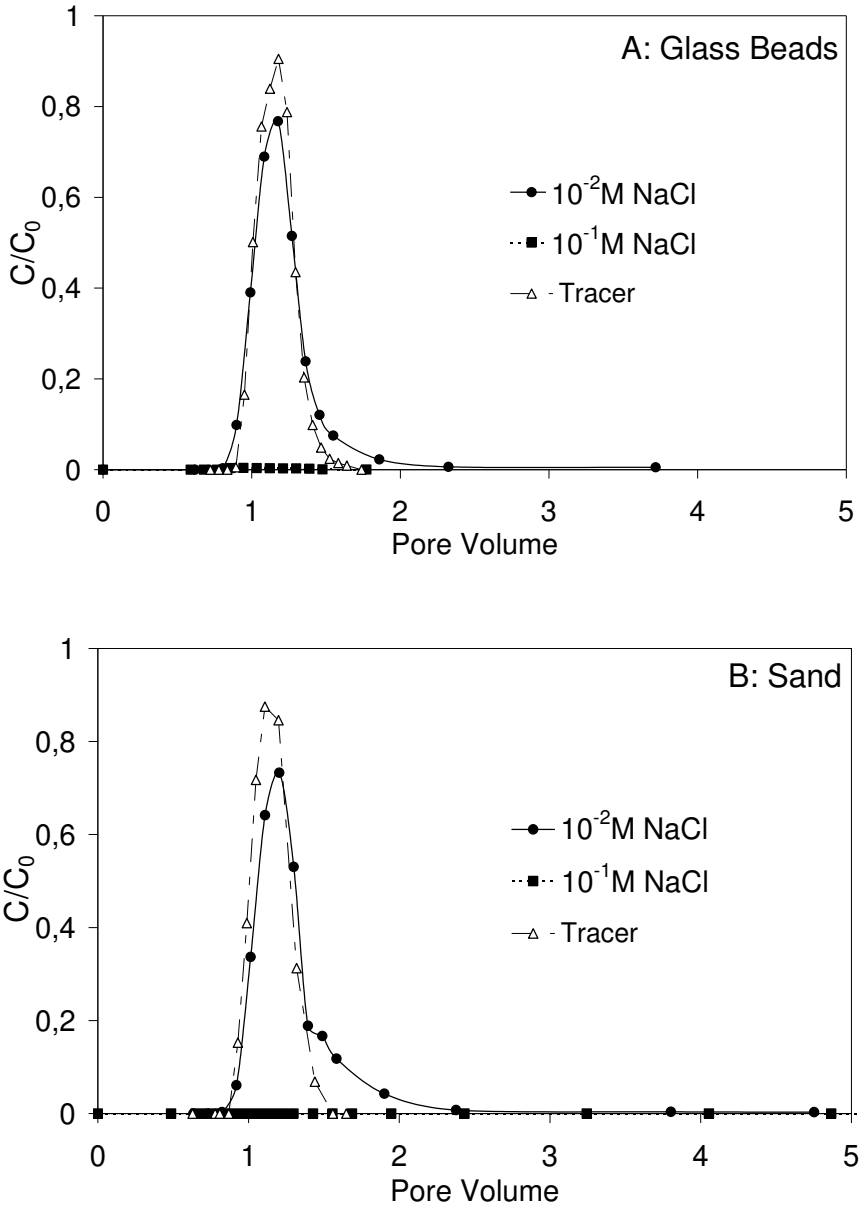

Figure 2: Effluent concentration curves for E. coli PHL1314 from (A) glass beads and (B) sand in two different ionic strengths.

Relative effluent concentrations of bacterial cells (C/C0) are plotted as a function of pore volumes. Tracer corresponds to effluent of bromide.

3. Results and discussion

3.1. Ionic strength and electrostatic repulsions

Both the PHL1314 strain and the porous media studied showed negative potential zeta values in all the ionic solutions (see table 2). Zeta potentials of the sand grains and the glass beads were nearly the same whatever the IS. The Gibbs free energies of interaction (i.e. $G^{EL} + G^{LW}$) between the sand and the PHL1314 cells as a function of distance and ionic strength was calculated using the classical DLVO theory (see figure 1). In the highest ionic conditions (10^{-1}M NaCl, pH7) electrostatic repulsions between the bacteria and the porous media were the lowest (404kT). Lowering the IS causes a decrease of the zeta potential of both the cells and the porous media and consequently an increase of electrostatic repulsions. At 10^{-4}M NaCl electrostatic repulsions were the highest (2300kT). Lowering the IS also increased the range of electrostatic interactions from 4nm at 10^{-1}M NaCl to 350nm in 10^{-4}M NaCl solutions. The secondary minimum provided by LW interactions was extremely weak compared to the electrostatic barrier and ranged from -3.69kT to -0.04kT. Moreover increasing the electrostatic barrier when the IS was decreased caused the secondary minimum to be attenuated (see figure 1).

3.2. Breakthrough curves

For both porous media studied ionic strength was a main factor for transport behavior of the PHL1314 strain and results are listed in table 3. In a 10^{-1}M NaCl solution transport of the PHL1314 strain was negligible for both the sand and the glass beads. In 10 fold lower ionic conditions the cells were significantly better transported: 89.8% (SD=2%) on the sand and 94.9% (SD=4%) on the glass beads. The bacteria breakthrough peak approximatively corresponded to the breakthrough peak of the tracer and was similar for the sand and the glass columns (about 1 pore volume, see figure 2).

To further investigate the influence of electrostatic interactions on bacterial adhesion in porous media the ionic strength was progressively decreased inside the column by

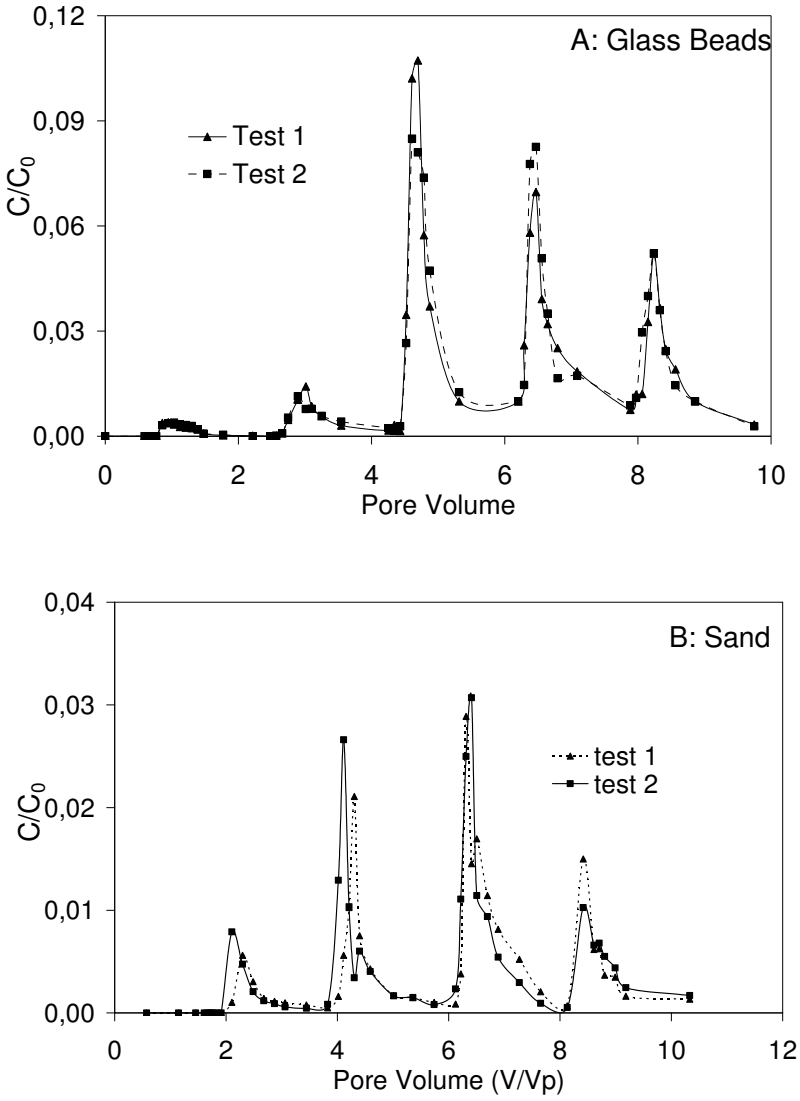

Figure 3: Bacterial breakthrough from (A) glass beads filled column and (B) sand filled column as lower ionic strength incoming solutions were injected.

The experiences were repeated two times.

injecting consecutively lower NaCl concentrated solutions starting at 10^{-1}M NaCl (pH remained constant at 7). Each time the IS was lowered variable amounts of bacteria cells were removed from the porous media (figure 3). The percentages of removed bacteria are given in table 3. Lowering the IS had a stronger effect in the glass beads column than in sand columns: 42% of the cells were released from the glass beads but only 18% from the sand matrix. Moreover it is interesting to notice that the amount of removed cells varied with the IS of the incoming solutions. Bacterial detachment was much better using the 10^{-3}M or 10^{-4}M solutions than with the 10^{-2}M solution (figure 3 and table 3). However lowering the IS does not enable to transport as many cells as with a low ionic solution on its own: for example 89% of the cells were transported through sand with a 10^{-2}M solution whereas only 2% of the cells traveled through the sand matrix when the IS was lowered from 10^{-1}M to 10^{-2}M (table 3).

3.3. Spatial and temporal fluorescens confocal imaging

3.3.1. Ionic strength impact

Bacterial transport through porous media was visualized using confocal microscopy. Figure 4 shows that bacterial adhesion on both the sand grains and the glass beads was much higher in a 10^{-1}M NaCl solution as it was also evidenced with the column experiments. In a 10^{-2}M solution only a few cells adhered to both porous media studied. Pictures shown in figure 4 were chosen as an example from among other essays with similar results. Even if the pictures from figure 4 were not taken from a same spot (since all experiences were performed independently) the impact of ionic strength was clearly observed. It is also interesting to notice that bacterial deposition occurred nearly systematically on the face exposed to the flow (figure 4).

The impact of lowering the IS on bacterial cell releasing inside the porous media was also analyzed with time lapse confocal imaging (see figure 5, supporting information). When the IS collapses suddenly due to the injection of distilled water in the flow cell, attached bacteria are released in the bulk fluid. Figure 6 shows the fluorescence intensity as a function of time during the IS lowering event. The fluorescence of attached cells was reduced by about 30%. It can also be seen from figure 5c that most of the bacterial cells could not be detached from the sand grains which is in agreement with our

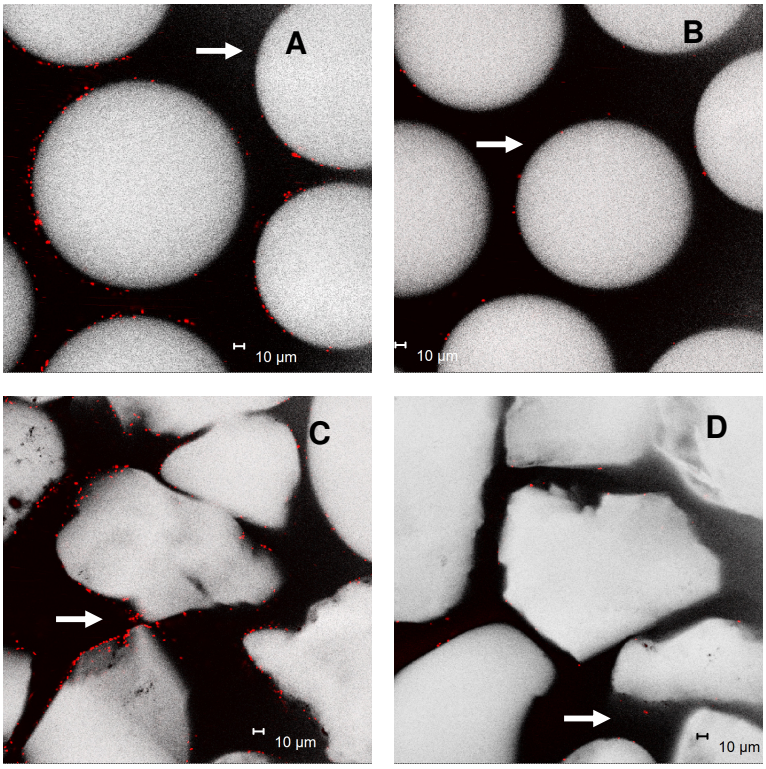

Figure 4: Bacterial adhesion in sand and glass beads media with two different ionic strengths after 15minutes:

(A) Glass beads 10^{-1}M NaCl (B) Glass beads 10^{-2}M NaCl (C) Sand 10^{-1}M NaCl (D) Sand 10^{-2}M NaCl. Pictures were taken 70µm inside the porous media at the end of the experiment (15minutes). Arrows indicate flow direction.

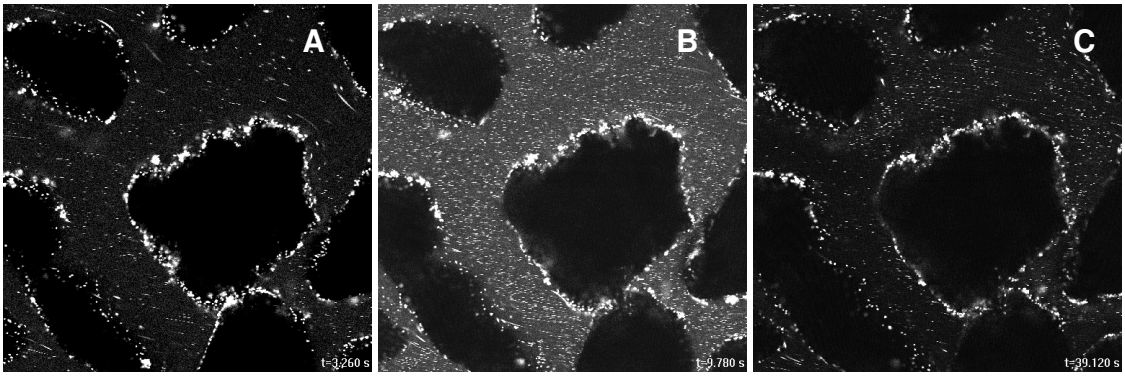

Figure 5: Time lapse bacterial detachment from a sand matrix by lowering the ionic strength (IS) visualized with a confocal microscope:

(A) Before the IS decreases (t=3sec.) (B) During the IS collapse (t=9sec.) (C) After the IS was decreased (t=39sec.).

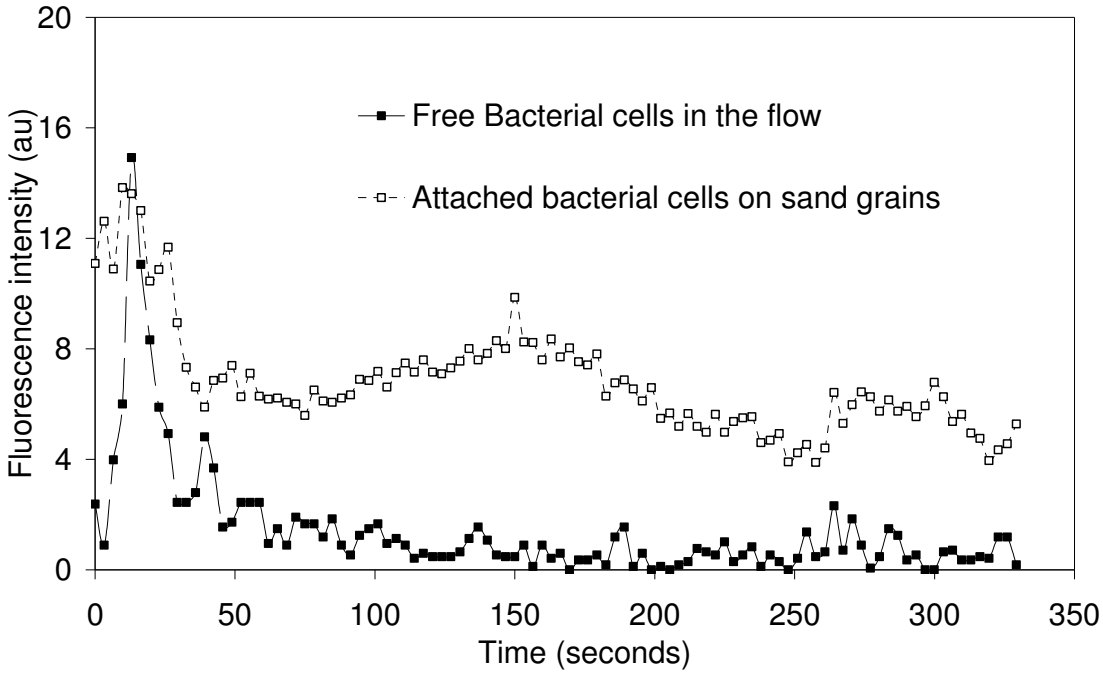

Figure 6: Fluorescence intensity (au) measured as a function of time for attached cells and free cells.

Measurements were performed using LSClite v2.5 software (Leica Microsystems, Germany) when distilled water was injected in the flow cell.

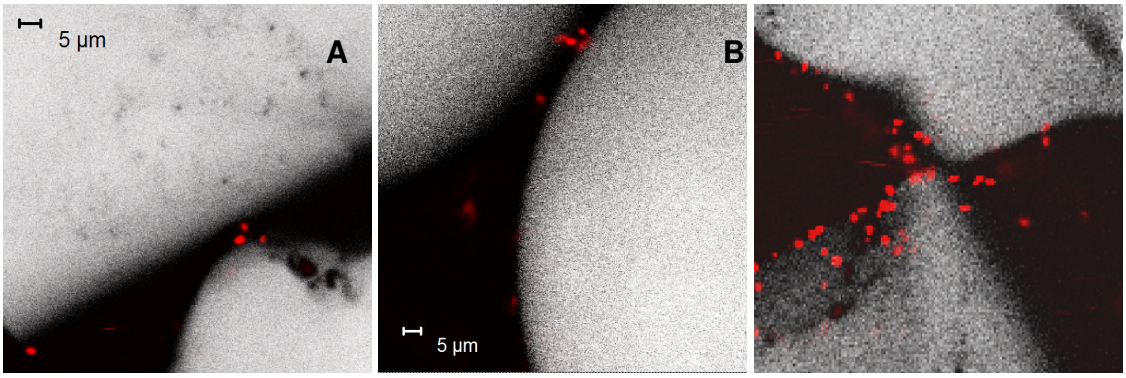

Figure 7: Wedging: examples of bacterial cells blocked by grain-grain junctions and narrow gates.

(A) Sand 10^{-2}M NaCl; (B) Glass 10^{-2}M NaCl; (C) Sand 10^{-1}M NaCl

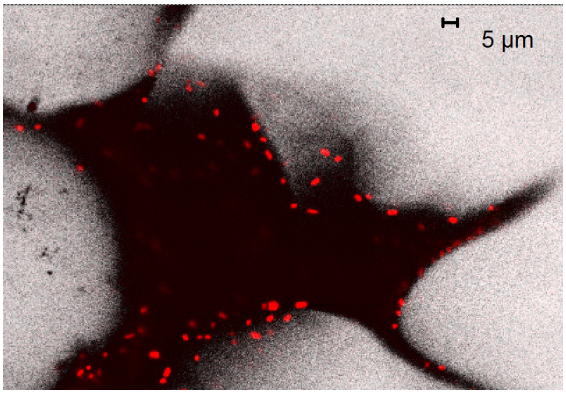

Figure 8: Example of *E. coli* PHL1314 cells trapped in a dead end path (sand matrix).

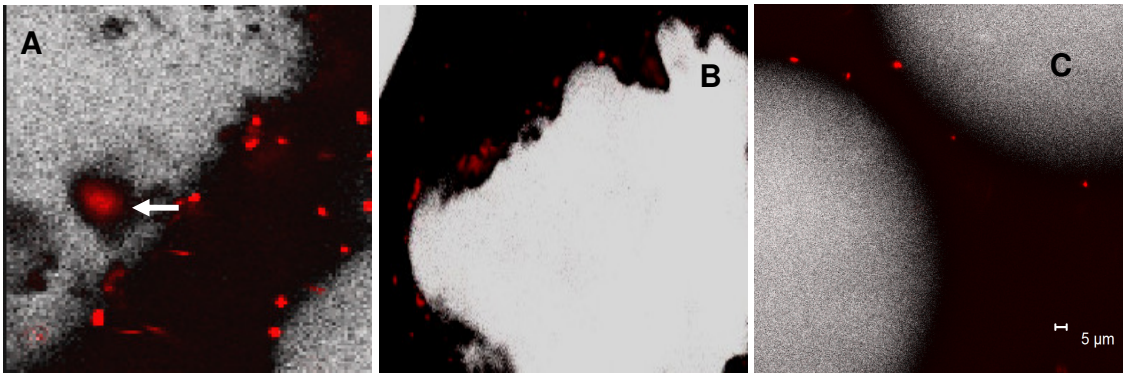

Figure 9: Bacterial cells retained by sand surface asperities as opposed to smooth characteristics of glass beads.

(A) Bacterial cell blocked in sand grain cavity (arrow) (B) bacterial cells retained inside sand grain asperities (C) Bacterial cells attached to smooth glass beads.

column experiments results (table 3). Similar results were observed for the glass beads (results not shown).

3.4. Porous media characteristics impact

Figures 7 to 9 illustrates how the matrix of a porous media can be responsible for blocking bacterial transport. Figure 7 is an example of wedging: bacterial cells blocked by grain-grain junctions and/or narrow gates inside the porous media. The phenomenon was visible in both the glass and the sand matrix but it seemed to happen more often in the sand media. Moreover higher ionic strength conditions seemed to enhance the blocking effect with an accumulation of cells resulting in a "traffic jam" (figure 7c). Figure 8 illustrates a dead end paths were the cells were trapped preventing their transport. Dead end paths were solely observed in the sand matrix but such structures were quite rare. Sand grain surface topography is rough showing cell-scale asperities and furrows were bacteria can be retained as figure 9a and 9b evidence. On the other hand glass beads are perfectly smooth spheres and thus are less likely to retain bacterial cells as they are simply deposited (figure 9c).

3.5. Drag torque calculations

The irregular shape of sand grains prevented us from calculating drag torque in the sand media as the equations only apply to model porous media such as packed glass beads. These calculations were performed according to the relationships given by Bergendahl and Grasso (Bergendahl et Grasso 2000) with a cell radius a_{cell} = 500nm ± 55nm (Cell size measurements were performed with a Canon BX microscope). The values of d_c, d_{max} and N_{pore} are listed in table 1 (see supporting information). Drag torque ranged from 3.35kT to 32.80kT which is sligly higher than LW interactions but much lower than EL intercations wich ranged from 404 to 2300kT. For the most part of the pore the drag force is lower than 10kT.

The transport of *E. coli* PHL1314 strain was largely impacted by ionic strength of the solution in both porous media studied. The PHL1314 strain is repelled from the collector's grain surface by an electrostatic barrier because both bacterial cells and porous media are negatively charged. Nearly opposite transport behaviors for the PHL1314

strain were observed at 10^{-1}M and 10^{-2}M ionic strength (table 3). At 10^{-1}M the electrostatic barrier of 404kT is only 4nm wide and LW interactions could act easily with a "deep" secondary minimum of -3.69kT creating favorable conditions for bacterial adhesion as is demonstrated by both column and confocal experiments. When the electrostatic barrier is very thin (like at 10^{-1}M) bacterial cells might come close enough to the solid surface so that either reversible attachment in a "deep" secondary minimum or irreversible attachment becomes possible (see figure 1, supporting information). On the contrary at 10^{-2}M the secondary minimum is less important (-1.08kT) and distance of closest approach increases dramatically (32nm thick electrostatic barrier) with less possibilities for bacterial deposition resulting in unfavorable conditions for bacterial retention in porous media. Differences between favorable and unfavorable conditions for bacterial retention in porous media were most likely due to the electrostatic barrier thickness as it not only increased separation distance from 4 to 32nm but also considerably reduced the secondary minimum depth. Moreover calculated minimum drag forces (3.39kT) were inferior to the secondary minimum depth at 10^{-1}M (-3.69kT) creating favorable possible conditions for bacterial retention while at 10^{-2}M drag forces overcome LW interactions (-1.08kT) worsening conditions for bacterial retention. It is interesting to notice that the mechanism of bacterial deposition is decided at only a few nanometers from the collectors grain surface which is very little when put in comparison with the size of bacterial cells.

To know in what proportion the bacterial cell population was either reversibly (i.e. secondary minimum) or irreversibly retained by both porous media studied in high ionic conditions (10^{-1}M) the IS was progressively lowered inside the columns. Bacterial detachment from both porous media studied resulted in very sharp breakthrough curves for each lower IS incoming solution (figure 3). These results suggest no dispersion occurred and that the detached cells migrated with the progression of the incoming solution through the columns. This can be evidenced from figure 6 which shows an important increase of fluorescence of the free cells in the flow when the distilled water runs throw the spot as witnessed in figure 5b: this excess of fluorescence corresponds to the bacteria which were released upstream from the spot and which progresses with the distilled water front through the sand matrix. As a result bacterial concentration increases suddenly and consequently the amount of fluorescence (figure 6). The amount of attached

cells diminished as the amount of fluorescence decreased just after the passage of the distilled water front. Interestingly the variable amount of cells detached for each incoming IS solution suggests the bacteria from a same population experience different level of interactions with the porous matrix (figure 3). Heterogeneity of the population or collector's grain surface may explain these results. Van der Mei and Busscher (2001) pointed out previously that the deviation calculated from individual electrophoretic cell measurements reflects a high degree of heterogeneity and may reveal the existence of subpopulations within a pure culture (van der Mei et Busscher 2001). If bacterial cells from a same population have different electrophoretic properties they will experience different EL and LW interactions with the porous matrix resulting in variable transport behaviors. Such heterogeneity in the bacterial population may explain why for each new incoming IS solution new portion of cells were released from the columns (figure 3). Other authors also suggested how cell membrane heterogeneity among a same bacterial population possibly affected bacterial transport through porous media (Liu *et al.* 2007; Simoni *et al.* 1998).

Bacterial cells were released from the porous media when the IS of the solution decreased (figure 3). Redman *et al.* obtained similar results although they used only a 10^{-3}M solution to decrease ionic strength (Redman *et al.* 2004). The authors concluded that the released bacterial cells were previously retained by LW interactions, referred as the secondary minimum. It should be kept in mind that as the electrostatic barrier thickens (i.e. when IS decreases) and moves the cells away from the surface, at the same time the LW interactions weaken (figure 1). As a result bacterial cells might be released because the secondary minimum becomes too weak to ensure bacterial retention. Moreover the minimum calculated drags forces (3.39kT) overcome LW interactions (<1kT) in low ionic strength and may help for cells to be released. Several authors pointed out the importance of hydrodynamic drag on colloid deposition and detachment in porous media environments (Li *et al.* 2005) ((Bergendahl et Grasso 2000). Theoretically since drag forces were far superior to LW retention forces in low ionic strength solutions all the bacterial cells retained in the secondary minimum should have been released. However increasing electrostatic interactions was not enough to recover completely the cells initially injected: only 40% of the bacteria were recovered from the glass matrix and 18% from the sand matrix. Hence, it seems that most of the cells were not retained in the

secondary minimum. On one hand our drag force calculations do no include zones of flow stagnation were bacterial cells could be retained as Johnson and colleagues recently pointed out (Johnson *et al.* 2007). On the other hand the cells which could not be released by lowering the IS might be irreversibly attached due to higher energy of interaction with the solid surface than those presented here. Using atomic force microscopy (AFM) measurements Cail and colleagues showed that interactions energy could be largely underestimated by classical DLVO equations (Cail et Hochella 2005). Interestingly, they used a solid phase and cells similar to ours and measured large (<0 attractive) interaction forces *once* cells are attached on the surface, which may explain why not all the cells could be detached from the porous matrix. Moreover omitting nanoscale surface roughness can lead to approximate DLVO calculations and LW interactions to be underestimated (Bhattacharjee *et al.* 1998). Nanoscale roughness is usually omitted for practical reasons but might not be neglected as several authors pointed out (Bhattacharjee *et al.* 1998; Hoek et Agarwal 2006; Hoek *et al.* 2003).

Confocal microscope observations revealed porous media geometry also affected transport of the PHL1314 strain. Two times more cells were detached from the glass media than from the sand grains despite similar characteristics (zeta potential, pore size, homogeneity…). Glass beads and sand grains mainly differ from their respective surface geometrical shape. Bradford *et al.* pointed out how bacterial transport can be hindered due to cell blocking by grain-grain junctions *(Bradford et al. 2006)*. Such junctions are probably more current in a sand matrix than in a glass beads matrix as sand grains are geometrically very irregular. As a result piled sand grains form a network of pore constrictions likely able to trap more bacteria than a matrix of perfectly spherical glass beads. Our confocal microscopy observations suggest mechanical trapping by porous media network of glass beads or sand grains with two types of retention: (i) wedging and straining at grain-grain junctions or narrow gates; (ii) blocking phenomena by surface asperities which only accounted for sand grains. Johnson and colleagues simulated colloids behaviour at a microscale in a porous media by means of a model accounting for the various forces experienced by the particles *(Johnson et al. 2007)*. They showed that colloid retention in presence of an energy barrier could happen due to wedging and retention in zones of flow stagnation (Johnson *et al.* 2007). The irreversibly retained bacterial cells found in our column experiments might be explained by their findings.

In summary *E. coli* PHL1314 transport was largely enhanced in low ionic strength environments. In soil environments ionic strengths are mostly very low and the pH is mild. Subsurface environments can thus be favourable for bacterial transport. These findings also showed the importance of porous media structure and geometry which modify bacterial transport behaviour. As a result geology of the soil can play an important role in preventing transport of pathogens towards drinking water sources. Moreover the experimental setup for *in situ* fluorescens time lapse confocal imaging was successful applied for our model, and may be used for other purposes.

Acknowledgements

This study was partly funded by the ADEME (French agency for Environment and Energy control) and the INRA (French National Institute for Agriculture Research). The authors would like to thanks the department of Essonnes for the financial support of a laser confocal microscope (ASTRE n°A02137).

4. Illustrations supplémentaires :

Les expériences réalisées au microscope confocal (voir Annexe 4 p. 259) ont permis de faire un très grand nombre de films et de photos dont certaines sont présentées ici. Le but de ces expériences était de visualiser l'attachement et le détachement des cellules d'*E. coli* PHL1314 dans deux milieux poreux différents : le sable et les billes de verre.

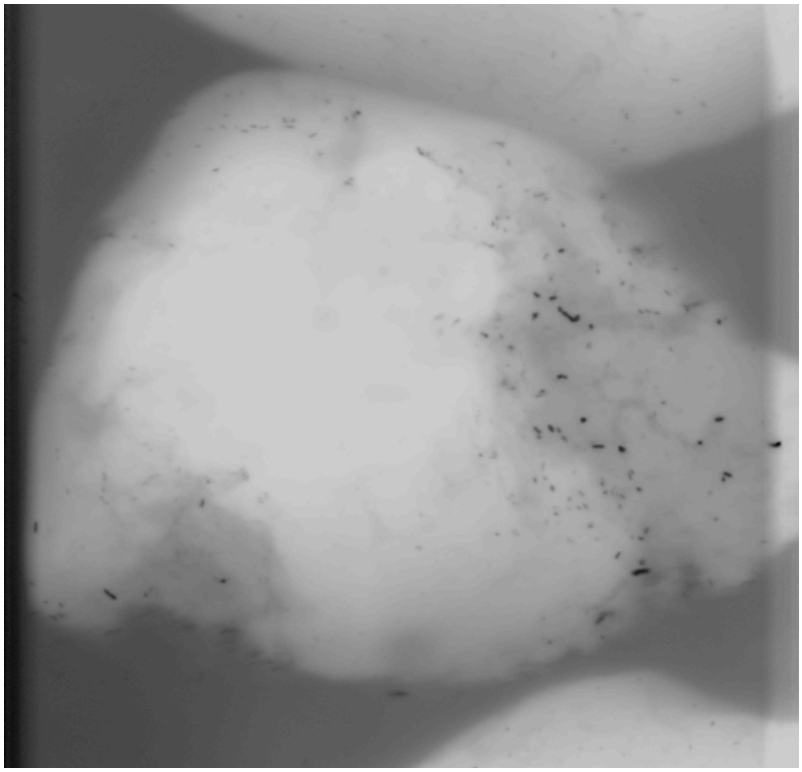

Figure 10 : Un grain de sable avec ses crevasses à la surface dans lesquelles des bactéries (tâches noires) sont piégées.

Cette image en 3D a été reconstituée par ordinateur à partir de coupes 2D empilées perpendiculaires à l'axe z.

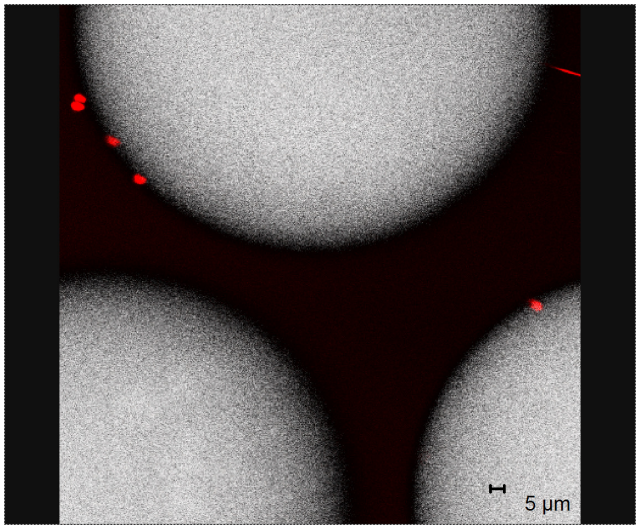

Figure 11 : Cellules d'*E. coli* PHL1314 « collées » à la surface de billes de verre.

(Force ionique du milieu : 10^{-2} M NaCl)

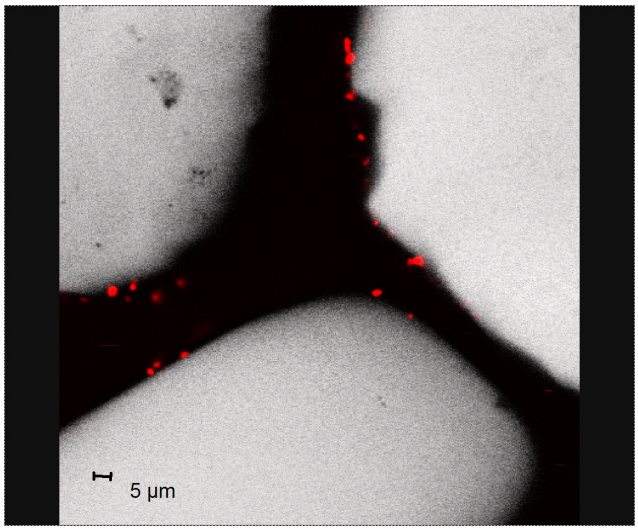

Figure 12 : Photo prise pendant le transport dans le sable d'*E. coli* PHL1314 montrant une zone en forme de fourche.

Ce type de zone semble favorable à l'adhésion des cellules sur les parois du milieu poreux.

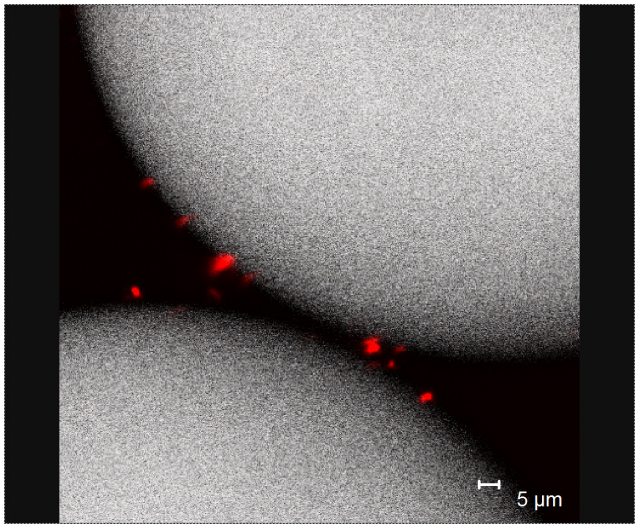

Figure 13 : Illustration du blocage de cellules au niveau d'une zone de contact entre 2 billes de verre.

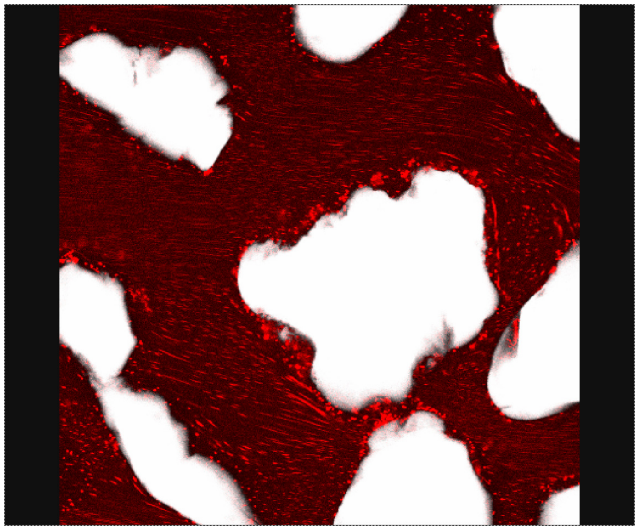

Figure 14 : Illustration des trajectoires et des vitesses de déplacement des cellules bactériennes dans un sable.

Il s'agit d'une photo dont le temps de prise est de plusieurs secondes ce qui explique les effets de traînées. Chaque traînée correspond à une cellule. Les vitesses de courant sont d'autant plus rapides que l'on s'éloigne de la surface des grains.